Published in final edited form as:
Dev Biol. 2007 December 1; 312(1): 217–230.

NOGGIN IS REQUIRED FOR NORMAL LOBE PATTERNING AND DUCTAL BUDDING IN THE MOUSE PROSTATE

Crist Cook[1,†], **Chad M. Vezina**[2,†], **Sarah M. Hicks**[2], **Aubie Shaw**[1], **Min Yu**[1], **Richard E. Peterson**[2], and **Wade Bushman**[1,*]

1*University of Wisconsin Department of Surgery*

2*University of Wisconsin School of Pharmacy*

Abstract

Mesenchymal expression of the BMP antagonist NOGGIN during prostate development plays a critical role in pre-natal ventral prostate development and opposes BMP4-mediated inhibition of cell proliferation during postnatal ductal development. Morphologic examination of newborn *Noggin*$^{-/-}$ male fetuses revealed genitourinary anomalies including cryptorchidism, incomplete separation of the hindgut from the urogenital sinus (UGS), absence of the ventral mesenchymal pad and a complete loss of ventral prostate (VP) budding. Examination of lobe-specific marker expression in the E14 *Noggin*$^{-/-}$ UGS rescued by transplantation under the renal capsule of a male nude mouse confirmed a complete loss of VP determination. More modest effects were observed in the other lobes, including decreased number of ductal buds in the dorsal and lateral prostates of newborn *Noggin*$^{-/-}$ males. BMP4 and BMP7 have been shown to inhibit ductal budding and outgrowth by negatively regulating epithelial cell proliferation. We show here that NOGGIN can neutralize budding inhibition by BMP4 and rescues branching morphogenesis of BMP4-exposed UGS in organ culture and show that the effects of BMP4 and NOGGIN activities converge on P63^{+} epithelial cells located at nascent duct tips. Together, these studies show that the BMP-NOGGIN axis regulates patterning of the ventral prostate, regulates ductal budding, and controls proliferation of P63^{+} epithelial cells in the nascent ducts of developing mouse prostate.

Keywords

Urogenital sinus; development; Noggin; Bmp; prostate

INTRODUCTION

The mouse prostate is a male accessory sex organ comprised of three distinct lobes: The coagulating gland (CG, also known as the anterior prostate), dorsolateral prostate (DLP), and ventral prostate (VP). The prostate develops from the urogenital sinus (UGS), a hindgut derivative of endodermal origin (Staack et al., 2003). The first morphological sign of prostate development is outgrowth of UGS epithelium into the surrounding UGS mesenchyme at sites which correspond to the origin of the three adult prostate lobes (Cunha et al., 1987). This process, which generates the main ducts of the adult prostate lobes, is initiated at embryonic

*Correspondence: Dr. Wade Bushman, University of Wisconsin-Madison, Department of Surgery, Box 3236 Clinical Science Center-G5, 600 Highland Ave., Madison, WI 53792, Phone (608) 265-8705, Email: bushman@surgery.wisc.edu.
†Authors contributed equally to this work.

day (E)16 in response to androgen stimulation and depends upon signaling interactions between UGS epithelial and mesenchymal layers. A variety of growth and signaling factors play important roles in prostate ductal budding and differentiation. These factors include sonic and indian hedgehog (SHH and IHH), fibroblast growth factor 10 (FGF10), bone morphogenetic proteins (BMP) 4 and 7, transforming growth factor β, notch1, nk3 homeobox 1, and forkhead box a1. Some of these factors promote epithelial proliferation and prostatic bud initiation, elongation, and branching morphogenesis (Almahbobi et al., 2005; Berman et al., 2004; Doles et al., 2006; Donjacour et al., 2003; Freestone et al., 2003; Gao et al., 2005; Huang et al., 2005; Lamm et al., 2002; Pu et al., 2004; Signoretti et al., 2005; Signoretti et al., 2000; Thomson, 2001; Thomson and Cunha, 1999; Tomlinson et al., 2004; Wang et al., 2006; 2004). Others inhibit epithelial cell proliferation and restrict prostate budding and branching (Grishina et al., 2005; Lamm et al., 2001). These signaling factors likely exert concerted and complementary actions to initiate bud initiation and outgrowth. However, significant uncertainty persists about the mechanisms which regulate the different signaling pathways, how growth regulation is tied to androgen-dependence of prostatic budding, and how positive and negative growth signals are choreographed to produce focal growth at the tip of emerging buds.

Prior to the initiation of prostatic budding, uniform *Bmp4* mRNA expression in UGS mesenchyme mirrors expression of *Shh* in the UGS epithelium. At the onset of ductal budding, *Bmp4* expression is diminished at the tips of buds while *Shh* expression localizes to nascent buds (Lamm et al., 2002; 2001). *Bmp4* expression subsequently diminishes throughout UGS mesenchyme except for tight rings of expression surrounding emerging buds. We postulated that down-regulation of BMP4 activity at sites of bud formation provides for localized de-repression of epithelial proliferation that produces outgrowth of the bud; however, the mechanisms regulating BMP4 expression or activity were unclear. More recent studies have shown *Bmp7* is expressed in both the mesenchyme and epithelium of the developing prostate and, like *Bmp4*, appears to inhibit epithelial proliferation, ductal budding and branching (Grishina et al., 2005). The effects of BMP4 and BMP7 on epithelial proliferation are likely to be a direct effect of the BMP ligands, however, the genes encoding the type I BMP receptors *Bmpr1a* and *Bmpr1b* are expressed in the mesenchyme as well as in epithelium, making paracrine mechanisms also possible. Also like *Bmp4*, *Bmp7* expression decreases in the mesenchyme adjacent to the duct tip. NOGGIN, a secreted factor which binds the BMP ligand in extracellular regions and prevents it from signaling through its receptor (Zimmerman et al., 1996), is critical for normal organogenesis as evidenced by defects in neural tube, somite, and skeletal development and lethality of *Noggin*$^{-/-}$ mutants (McMahon et al., 1998; Smith, 1999). A critical role of NOGGIN in opposing and balancing BMP4 activity is demonstrated by a partial rescue of the *Noggin*$^{-/-}$ phenotype by *Bmp4* haploinsufficiency (Wijgerde et al., 2005). We report here that the BMP-antagonist *Noggin* is expressed in mouse UGS mesenchyme and is required for patterning ventral prostate development. In addition, we show that NOGGIN neutralizes inhibition of epithelial proliferation by BMP4 and postulate that the opposing actions of BMP4 and NOGGIN specify sites of ductal budding and regulate bud outgrowth.

MATERIALS AND METHODS

Tissue Collection

CD-1 timed-pregnant mice (Charles River, Willmington, MA) were euthanized by isoflurane overdose. The day of plug was considered E0. UGS from E14-18 and prostate from postnatal day (P) 1, 5, and 10 male mice were dissected in Dulbecco's phosphate-buffered saline (PBS). For RT-PCR, UGS specimens were snap frozen in liquid N_2 and stored at −80°C. For UGS organ culture, the seminal vesicles and bladder were excised and the UGS was temporarily

stored in ice-cold PBS until culture initiation. For scanning electronic microscopy, UGS tissue was either stored in 10% FBS in Hank's Balanced Salt Solution (HBSS) overnight at 4°C or processed immediately.

RNA Isolation and RT-PCR

RNA was isolated from pooled UGS (*n* = 6-9 E14-18 male fetuses from multiple litters) or individual prostate tissue from P1-P10 male neonates. Specimens were homogenized in Molecular Grinding Resin™ (Genotech, St. Louis, MO) and tissue homogenates were passed through Qiashredder columns (Qiagen, Valencia, CA). RNA was extracted from tissue homogenates with the Qiagen RNeasy kit (Qiagen). Reverse transcription was carried out for 1 hour at 42°C in 1X First stand buffer containing 500 ng total RNA, 0.5 μM dNTPs, 150 ng random hexamers, 5 mM DTT, and 200 U Superscript II Reverse transcriptase (Invitrogen, Carlsbad, CA). Real-time PCR was performed as described previously (Lin et al., 2003) using the Roche LightCycler (Roche Molecular Biochemicals, Indianapolis, IN). PCR primers used in this study are listed in table I.

UGSM-2 Cell Line

The immortalized UGS mesenchymal clonal cell line (UGSM-2) was generated from a parent mixed cell population derived from the UGS of an E16 male $INK4a^{-/-}$ transgenic mouse embryo (Shaw et al., 2006). For gain of function studies, UGSM-2 cells were transfected with a Noggin/GFP bi-citronic expression vector. 8×10^6 *wild-type* (WT) UGSM-2 cells or UGSM-2 Noggin over-expressing cells were combined with minced P1 WT prostate tissue, allowed to recombine overnight in organ culture, and grafted under the renal capsule for 3 weeks.

Whole Mount *In-Situ* Hybridization

UGS and prostate tissue were fixed in 4% paraformaldehyde and hybridized according to a previously described protocol (Lamm et al., 2001). Briefly, tissues were bleached for 60 minutes in 6% H_2O_2 and digested with 50 μg/ml proteinase K for 30 minutes at room temperature. Prehybridization (2 hours) and hybridization (overnight) were each performed at 68°C. After high stringency washes, tissues were incubated at 4°C overnight with pre-blocked alkaline phosphatase-conjugated anti-digoxygenin. The colorimetric reaction used nitroblue tetrazolium and 5-bromo-4-chloro-3-indoyl phosphate as chromagens. Cryosections were prepared after overnight equilibration in 50% sucrose.

Assay for β-Galactosidase Activity

β-Galactosidase activity was determined, as an indirect measure of *LacZ* expression, by enzymatic cleavage of X-gal (5-bromo-4-chloro-3-indolyl-β-D-galactoside) as described (Cheng et al., 1993). UGS specimens were fixed for 20 minutes in ice cold 4% paraformaldyde, rinsed with PBS, and suspended in PBS containing 5 mM $K_3Fe(CN)_3$, 5 mM $K_4Fe(CN)_6$, 2 mM $MgCl_2$, 0.02% NP-40, 0.01% sodium deoxycholate, and 1 mg/ml X-gal. Tissues were incubated for 30 minutes at 37°C in the dark on a rocking platform, washed with PBS, and imaged by light microscopy. Cryosections were prepared from these specimens for further analysis.

In Vitro Organ Culture

E14 UGS or P1 prostate were grown as previously described (Doles et al., 2005). Experimental supplements included recombinant mouse NOGGIN (1 μg/ml, R&D Systems, Minneapolis, MN), recombinant human BMP4 (300 ng/ml, R&D Systems), octylated SHH (5 nM, Curis, Cambridge, MA), or cyclopamine (10 μM; Toronto Research Chemicals, Toronto, Canada). Organ culture media was replenished every 48 hours.

Transgenic Mice

A breeding pair of *Noggin*$^{tm1(Lacz)Am}$ mice that was first described by the McMahon lab (McMahon et al., 1998) was obtained with permission from Brigid Hogan (Duke University). The *LacZ* open reading frame was targeted to the first exon of *Noggin* and the remaining gene sequence, except for a small portion of the 3'-terminus, was excised to generate the mutant allele. The *Noggin* mutant mice described by McMahon were maintained on a C57BL6/J background but are now out-crossed with ICR mice. *LacZ* primers (Forward: ACC CAA CTT AAT CGC CTT GC; Reverse: AAC AAA CGG CGG ATT GAC C) identified the genotype of the offspring. *Noggin*$^{-/-}$ tissue was obtained from male fetuses during in utero development or at day of birth. A breeding pair of *Gremlin*$^{+/-}$ (*Grem1*^{tm1Rmh}) mice that was first described by Khokha et al. (2003) was provided with permission by Dr. Xin Sun (University of Wisconsin). A breeding pair of *Chordin*$^{+/-}$ (*Chrd*^{tm1Emdr}) mice was provided by the Edward DeRobertis lab (UCLA), and was maintained on a mixed B6SJLF1/JxC57Bl/6J background.

Renal Grafts

UGS were dissected, cleaned, and seminal vesicles removed. The tissue was stored in cold Hank's Buffer until surgical implantation under the renal capsule of CD-1 nude male mice that were at least 8 weeks of age as described (http://mammary.nih.gov/tools/mousework/Cunha001/index.html). After 3 weeks, UGS grafts were removed from their hosts. For each host mouse, half of each graft was fixed in 10% formalin for histology and the other half was snap frozen for RNA analysis.

Scanning Electron Microscopy

E17 UGS specimens were partially digested with 1% trypsin in HBSS for 90 minutes at 4°C. UGS epithelium was mechanically separated from UGS mesenchyme then processed, mounted, and imaged by scanning electron microscopy as described previously (Lin et al., 2003).

Immunofluorescence and Immunohistochemistry

UGS and prostate tissue sections were de-paraffinized, hydrated, and processed for antigen retrieval (Garrett, 1998). UGS sections were incubated for overnight at room temperature in a blocking buffer containing anti-P63 rabbit polyclonal antibody (1:100, Santa Cruz Biotechnology Inc., Santa Cruz, CA). UGS sections were rinsed briefly and incubated for 1 hour at RT with blocking buffer containing Alexa Flour 546 or 488 conjugated goat anti-mouse IgG (1:200, Invitrogen). Sections were DAPI counterstained, cover-slipped, and imaged. To visualize proliferating cells, 5-bromo -2'-deoxyuridine (BrdU) labeling medium was added to the organ culture media (1:1000 v/v, Roche Applied Science) 4 hours prior to fixing the UGS tissue or injected (1 ml undiluted per 100 g body weight, *i.p.*) into mice 2 hours before euthanasia. BrdU positive cells were labeled according to the manufacturer's protocol. BrdU-positive proliferating cells (percent of total cells) were counted from 3-6 sections from each UGS (4 UGS per genotype), using a fixed area from a 200X magnification field. To examine the effect of BMP4 and NOGGIN on cell proliferation, 2 to 6 images, and 13 to 51 ducts were identified in each of 16 UGSs (four UGSs per treatment group). Within each duct, we counted the numbers of (P63+,BrdU+); (P63+,BrdU-); (P63-,BrdU+); and (P63-,BrdU-) epithelial cells and calculated the ratios P63+,BrdU+)/(P63+,BrdU-) and (P63-,BrdU+)/(P63-,BrdU-) to determine the mitotic index among P63+ and P63- epithelial cells, respectively. We compared these ratios across treatment groups using an analysis of variance with a random mouse effect to account for the repeated measurements taken from the same animal. We used an arcsin-square-root transformation of the ratios in order to better meet the assumptions of the analysis. Pair-wise comparisons were made using Fisher's protected least significant difference tests when the overall treatment effect was significant. P-values less than 0.05 were considered as

significant. All analyses were performed using SAS statistical software version 9.1, SAS Institute Inc., Cary, NC.

RESULTS

Localization of *Noggin* expression in the developing male UGS and prostate

Abundance and localization of *Noggin* mRNA during prostate development was determined by a combination of real-time PCR, in-situ hybridization and assessment of β-galactosidase activity in *Noggin*$^{+/-}$ mice that expressed *LacZ* under the control of the *Noggin* promoter. *Noggin* expression was restricted to UGS mesenchyme, was most abundant prior to the onset of prostatic budding (E14-E16) and then decreased gradually during bud elongation (E17-P1) and postnatal prostate morphogenesis (Fig. 1A). Mesenchymal *Noggin* expression extended from the bladder neck through the UGS and urethra at E14 (not shown) and E16 (Fig. 1B, left, top row). Later in development, *Noggin* expression localized to a thin band of mesenchyme peripheral to the nascent smooth muscle layer. *Noggin* expression contoured nascent buds and its expression domain around buds was expanded and concentrated distally towards bud tips (Fig. 1B, middle row). *Noggin* expression at P5 and P10 remained tightly associated with the ductal network of the developing prostate (Fig. 1B, bottom row). *Noggin* expression in the adult prostate was very low (not shown).

Regulation of *Noggin* expression

To examine the influence of SHH and BMP4 on *Noggin* expression, we utilized organ culture of the E14 male UGS in DHT-supplemented, serum-free media. Exogenous BMP4 significantly increased *Noggin* expression (Fig. 2A). This appears be a direct effect on UGS mesenchyme since BMP4 also induced *Noggin* expression in the UGSM-2 cells (Fig. 2B). *Noggin* expression in the cultured UGS was unchanged by the addition of exogenous SHH (Fig. 2A). However, RT-PCR analysis of SHH-responsive *Gli1* expression demonstrated considerable hedgehog (Hh) signaling activity in these cultured tissues in the absence of exogenous SHH and no significant increase with SHH treatment (results not shown). Since the effect of exogenous SHH on *Noggin* may be masked by robust constitutive Hh signaling, we examined the effect of the Hh inhibitor cyclopamine on *Noggin* expression (Fig. 2A). Chemical blockade of Hh signaling by cyclopamine produced a marked increase in *Noggin* mRNA abundance, suggesting that Hh signaling actually represses *Noggin* expression. Since studies examining the effect of *Shh* and cyclopamine on *Noggin* expression in the UGSM-2 cell line revealed no direct effects (not shown), we infer that the effect of Hh signaling on *Noggin* expression may be context-dependent or require cross-talk between the UGS epithelium and mesenchyme.

Phenotype of developing mouse urogenital tract from *Noggin*$^{-/-}$ male mouse fetuses is abnormal and unique from *Chordin*$^{-/-}$ and *Gremlin*$^{-/-}$ male fetuses

Noggin$^{-/-}$ mice have been previously reported to exhibit stunted growth, lack of cranial fusion, shortened limbs, a complete loss of lumbar skeletal and tail formation, and perinatal lethality (McMahon et al., 1998; Smith, 1999). However, development of the urogenital system in these mice has not been previously described. In our study of male *Noggin*$^{-/-}$ mouse fetuses, we observed a constellation of urogenital abnormalities including an occasional pelvic kidney, and variable degrees of cryptorchidism ranging from a high intra-abdominal position to complete descent. Some males exhibited agenesis of the membranous (pelvic) urethra, others developed a precursor urethral epithelial tube, and some exhibited agenesis of the bulbourethral gland. The most striking abnormalities were incomplete separation of the hindgut from the UGS and agenesis of the tail. Separation of the hindgut from the UGS normally occurs at E13 when endodermal lined mesenchymal Rathke folds, which flank the UGS laterally, fuse medially to create the urorectal septum (Hynes and Fraher, 2004). Whereas E17 WT males exhibited a

complete separation of the UGS and hindgut, the E17 *Noggin*$^{-/-}$ male exhibited a fistulous connection between the hindgut and the dorsal surface of the UGS (Fig. 3A). This was typically associated with anal atresia. The E17 *Noggin*$^{-/-}$ female exhibited a similar defect (not shown).

Scanning electron microscopy was performed on E17 *Noggin*$^{-/-}$ and WT UGS tissues (n = 3 per genotype) in which the epithelium was mechanically separated from UGS mesenchyme in order to provide high resolution imaging of the ductal budding pattern. The isolated E17 WT UGS epithelium exhibited a prominent dorsal sulcus, or groove, formed by two ridges from which the dorsal UGS buds emerge (Fig. 3B, dorsal buds are pseudo-colored green). Lateral prostatic buds (yellow) emanated from the lateral surfaces flanking the sulcus. The seminal vesicle (SV) and ductus deferens (DD) drained into the ejaculatory duct located within the dorsal sulcus and caudal to the prostatic utricle (PU). CG buds (red) and VP buds (blue) were located cranial to the ejaculatory duct. The bladder neck was positioned at a right angle to the urethra and the VP, lateral, and CG buds formed at discrete sites along the prostatic urethra immediately caudal to its connection to the bladder neck (Fig. 3B, right, top row). The E17 *Noggin*$^{-/-}$ UGS appeared somewhat smaller and exhibited several distinctive abnormalities. The characteristic dorsal ridges were absent or reduced in size, resulting in loss of the dorsal sulcus and exposure of the ejaculatory duct connection. The angulation of the bladder neck - urethral axis was considerably more obtuse. Most striking was the total absence of VP and CG buds in all three *Noggin*$^{-/-}$ UGS samples examined (Fig. 3B, right, bottom row). The number of dorsal and lateral buds was also reduced but a complete absence of ductal budding was not observed in any of the *Noggin*$^{-/-}$ UGS specimens.

Two other BMP antagonists, *Gremlin* and *Chordin*, are also expressed in the UGS during prostatic bud initiation (results not shown). In contrast to *Noggin*, however, they do not appear to play an essential role in normal prostatic budding. When we examined *Gremlin*$^{-/-}$ and *Chordin*$^{-/-}$ mice several days after prostatic bud initiation (Fig. 3C), the budding patterns and bladder neck - urethra angle appeared indistinguishable from WT male littermates.

To exclude the possibility or occult hypogonadism in the *Noggin*$^{-/-}$ mouse, we utilized previously described functional assays of testis androgen production (Donjacour et al., 2003). First, E15-16 WT and *Noggin*$^{-/-}$ UGS tissues were cultured together with their respective testes in (-) DHT, serum-free organ culture for 7 days. The UGS tissues exhibited comparable degrees of budding, indicating sufficient androgen production by the *Noggin*$^{-/-}$ to induce budding. Second, the WT P1 prostate was cultured in androgen-free, serum-free organ culture alone or together with WT or *Noggin*$^{-/-}$ testes. WT tissues cultured alone showed minimal branching; whereas, the tissues cultured with WT and *Noggin*$^{-/-}$ exhibited similar degrees of branching morphogenesis (Supplemental Figure 1).

Noggin is required for formation of the ventral mesenchymal pad and for ventral UGS epithelial cell proliferation

Signals from UGS mesenchyme play an integral role in initiating androgen-dependent prostatic buds from the UGS epithelium. UGS mesenchyme is thought to possess regionally patterned inductive capacities that determine the identity of the different prostate lobes and induce epithelial proliferation and bud initiation (Hayashi et al., 1993). Abnormal UGS mesenchymal development is one possible mechanism for deficient bud formation in *Noggin*$^{-/-}$ UGS. Consistent with this hypothesis, we observed a reduction in ventral mesenchyme thickness and density in P1 *Noggin*$^{-/-}$ prostate tissue sections (Fig. 4A, left column, outlined in pink). Decreased volume or possible agenesis of the ventral mesenchymal pad, a specialized UGS mesenchymal tissue compartment that is responsible for synthesis of FGF10 and other prostatic bud-inducing secretory proteins, may contribute to impaired epithelial cell proliferation and prostatic bud initiation.

Two days prior to prostatic bud initiation, the E14 *Noggin*$^{-/-}$ UGS showed diminished ventral mesenchymal cell density relative to the age-matched WT UGS (Fig. 4A, right column, outlined in pink), which is consistent with impaired ventral mesenchymal pad formation observed on P1. The decreased ventral mesenchymal cell density at E14 was accompanied by a significant decrease in ventral UGS epithelial cell proliferation (Fig. 4B, white arrowheads). These results indicate that unopposed BMP signaling may inhibit formation of the ventral mesenchymal pad and proliferation of ventral epithelium, thereby blocking ventral prostatic bud formation.

Selective loss of ventral prostate differentiation in *Noggin*$^{-/-}$ male mice

The absence of ventral buds and the ventral mesenchymal pad in the *Noggin*$^{-/-}$ UGS could reflect either altered patterning in lobar development, resulting in a true loss of VP determination, or an altered morphology of the UGS with VP identity shifted to a more dorsal position. Since the different lobes of the prostate are distinguished by the expression of lobe-specific markers, we sought to distinguish between these two possibilities by examining lobe-specific gene expression in mature prostate tissue of the *Noggin*$^{-/-}$ mutant. To circumvent the limitations of perinatal lethality in *Noggin*$^{-/-}$ mice and examine the requirement of *Noggin* for prostate development during early postnatal life, P1 WT and *Noggin*$^{-/-}$ male prostates were grafted under the renal capsule of adult male nude mice. The 3 week grafts were similar in size even though the P1 *Noggin*$^{-/-}$ prostate was approximately half the size of the WT prostate at the time of grafting. Histological examination of sectioned grafts from both genotypes revealed glandular morphogenesis consistent with prostatic differentiation (Fig. 5A), however, the *Noggin*$^{-/-}$ grafts were notable for the absence of any glands showing the characteristic VP glandular architecture. Real-time PCR was performed on mRNA from the grafts to assess relative abundance of prostatic differentiation markers. The specificity of spermine binding protein (*Sbp*) as a marker for VP, renin 1 (*Ren1*) for CG, and probasin (*Pbsn*) for DLP was confirmed using cDNA isolated from the various lobes of the P35 WT mouse prostate (Fig. 5B). Expression of the DLP (*Pbsn*) and CG (*Ren1*) markers in *Noggin*$^{-/-}$ grafts was not significantly different from WT grafts (Fig. 5B). However, expression of the VP-specific marker (*Sbp*) (Lin et al., 2003;Mills et al., 1987;Thielen et al., 2007) was absent from the *Noggin*$^{-/-}$ grafts.

In order to determine whether VP development in the *Noggin*$^{-/-}$ UGS could be rescued by exposure to exogenous NOGGIN prior to and during initiation of prostatic budding, E12 WT and *Noggin*$^{-/-}$ UGS were exposed to recombinant NOGGIN protein for 5 d in organ culture and grafted under the renal capsule for 21 d. Although UGS from WT mice were capable of forming ventral prostate tissue under these conditions, recombinant NOGGIN protein was unable to rescue ventral prostate development in *Noggin*$^{-/-}$ UGS (results not shown).

To determine whether *Noggin* haploinsufficiency would exert a ventral lobe-specific effect on postnatal prostate development, we compared prostate lobe size, histological appearance and branching complexity in WT and *Noggin*$^{+/-}$ mice. The VP weight from P35 *Noggin*$^{+/-}$ male mice was significantly less than that of age-matched WT controls ande there was no difference in the DLP or CG weights (Fig. 5C). Micro-dissection of the different prostatic lobes showed no significant differences between WT and *Noggin*$^{+/-}$ mice in the number of main ducts, branch points, or duct tips for any of the lobes and histological examination of each prostate lobe of adult *Noggin*$^{+/-}$ mice revealed no obvious abnormalities (results not shown).

Effect of NOGGIN on Budding

In order to determine the role of NOGGIN in prostatic budding, E14 UGS tissue was cultured for 7 days in DHT-supplemented control media or in media containing DHT and exogenous NOGGIN, BMP4, or both. Prostatic main ducts and bud tips were quantitated from light

micrographs (Fig. 6) as described previously (Lamm et al., 2001). NOGGIN exposure alone did not significantly alter the number of main prostatic ducts or bud tips compared to control UGS tissues and although NOGGIN appeared to increase outgrowth of buds in several different experiments, this difference was not amenable to quantitative analysis. As previously reported, BMP4-exposed UGS tissues exhibited fewer main ducts and bud tips (Almahbobi et al., 2005;Lamm et al., 2001) and concurrent exposure to NOGGIN+BMP reversed bud inhibitory actions of BMP4.

Ontogeny of P63 during prostate ductal morphogenesis

While prostate ductal morphogenesis has been extensively studied, the ontogeny of P63 expression during prostate development and its relationship to epithelial proliferation and ductal outgrowth has not been well characterized. The *p63* gene encodes multiple isoforms. The predominant isoform in epithelial tissues lacks the acidic N-terminus that is related to the transactivation domain of *p53* (Yang et al., 1998). P63 is required for prostatic bud development, may be expressed by precursors of differentiated secretory cells, and is expressed by basal cells of the adult prostate (Marker et al., 2003; Signoretti et al., 2005). Prior to the onset of prostate ductal budding, P63 was expressed throughout the multilayered epithelium of the UGS, with stronger staining at the epithelial-mesenchymal interface (Fig. 7A). During ductal budding, the nascent epithelial buds exhibited a nearly continuous sheath of P63+ cells at the epithelial-mesenchymal interface that surrounded a core of P63- epithelial cells (Fig. 7B). Later in development, the continuous sheath of P63+ cells persisted at duct tips but was discontinuous in elongating bud stalks and assumed a punctate basal epithelial distribution more characteristic of adult prostate ducts (Figs 7C, D). Double immunofluorescence staining for P63 and ki67 was performed to examine co-localization of P63+ cells with the proliferating cell population during ductal outgrowth. High magnification imaging of the buds in the P1 prostate showed P63+ cells lining the periphery of emerging buds (Fig. 7E, red staining) and active cell proliferation in bud epithelium and surrounding mesenchyme (Fig. 7E, Ki67 green staining). Ki67 expression co-localized with P63+ cells at the distal tips of emerging buds (Fig. 7E, yellow double-staining). P63+ cells in the proximal portion of buds were mitotically quiescent and proliferation was instead restricted to P63- cells in the periphery and center of non-canalized proximal segments.

NOGGIN stimulates a burst of proliferation in P63+ UGS epithelial cells following BMP4 exposure in UGS organ culture

To investigate how NOGGIN influenced the distribution of proliferating cells, P1 prostate tissue was cultured in DHT-supplemented media for 4 days ± addition of NOGGIN on day 3. Tissues were incubated with BrdU 4 hr prior to fixation to label mitotically active cells. P63+ and BrdU+ cells were identified by immunohistochemistry and quantified as described in the Materials and Methods. Control tissues displayed epithelial cell proliferation generally , concentrated toward the periphery of the tissue and localized primarily to bud tips. These proliferating cells included P63+ and P63- cells and the proliferation pattern was similar to that observed in vivo at P1. Preliminary studies showed that treatment with NOGGIN for four days in organ culture produced no obvious change in epithelial proliferation (unpublished observations). Recognizing that reciprocal regulatory relationships between *Bmp4* and *Noggin* or functional redundancy provided by other members of the BMP/NOGGIN family may frustrate our efforts to tease out the effect of the BMP4/NOGGIN axis on epithelial proliferation, we examined the influence of short-term NOGGIN exposure on epithelial proliferation following pre-treatment with BMP4. P63+ cells were localized to the outer edge of elongating ducts in prostate tissues that were cultured for 4 days in control media, and BrdU + proliferating cells were observed in both mesenchymal and epithelial tissue compartments (Fig. 8A). When tissues were cultured in control media for 3 days followed by treatment with NOGGIN for 1 day (Fig. 8B), there was no change in proliferation of either P63+ or P63- cells

compared to control tissues. Tissues cultured in the presence of exogenous BMP4 for 4 days exhibited significantly decreased proliferation of P63+ epithelial cells (Fig. 8C and E) but no change in the proliferation of p63- cells (data not shown). When tissues were treated for 3 days with BMP4 followed by treatment with NOGGIN for 1 day, there was an apparent burst of P63+ epithelial proliferation at the leading edge of the buds and ducts (Fig. 8D) and statistical analysis demonstrated that one day of NOGGIN treatment restored P63+ cell proliferation to control levels (Fig. 8E). There was no change in the proliferation in P63- cells (data not shown). These observations suggest that opposing actions of BMP4 and NOGGIN converge to regulate proliferation of P63+ epithelial cells in the nascent ducts of the developing prostate.

DISCUSSION

NOGGIN is an extracellular binding protein with high affinity for BMP4 and lesser affinity for BMP2, BMP7, and GDF5 (Balemans and Van Hul, 2002). Both *Bmp4* and *Bmp7* are abundantly expressed during prostate development while *Bmp2* is expressed at lower levels and *Gdf5* expression is virtually undetectable (Grishina et al., 2005; Lamm et al., 2001). Both *Bmp4* and *Bmp7* are expressed in the periurethral mesenchyme prior to bud formation (Grishina et al., 2005; Lamm et al., 2001). Once the prostate buds have formed, *Bmp4* expression is most abundant in the mesenchyme surrounding the proximal duct segment. *Bmp7* expression is diminished in the UGS mesenchyme surrounding prostatic bud tips while being increased in bud epithelia. Both have been shown to inhibit budding/branching in organ culture and the action of BMP4 has been linked to a selective inhibition of epithelial proliferation.

SMAD1 phosphorylation is a downstream marker for BMP receptor activation. Grishina et al. (2005) observed that phosphorylated SMAD1 expression was restricted to mouse urogenital sinus epithelium at E18, suggesting that the effect of the BMP ligands is a direct effect upon UGS epithelium. Supporting this inference are preliminary findings that expression of phosphorylated SMADs 1, 5, and 8 and the BMP4 responsive-gene, *Smad6,* are largely confined to the urogenital sinus epithelium (unpublished observations).

BMP4 regulates budding and branching morphogenesis in the developing lung by increasing expression of the cell cycle inhibitor *P21* and decreasing expression of *Cyclin D* and *Cdk2* (Jeffery et al., 2005). BMP7 is reported to control formation of new buds and branching morphogenesis in the prostate by regulating *Hes1*/*Notch1* expression domains (Grishina et al., 2005). Our studies lead us to postulate that NOGGIN acts to specifically inhibit BMP4/7 activity during ductal budding and at the distal tips of elongating prostatic buds to facilitate outgrowth and simultaneously create a gradient of BMP signaling along the ductal axis. These activities are suggested by our organ culture studies showing that exogenous NOGGIN expands proliferation of P63- cells specifically at the distal tips of developing prostatic buds and can reverse BMP4-induced inhibition of bud outgrowth. These effects of NOGGIN may be mediated by regulation of cell cycle genes and regulation of *Hes1*/*Notch 1* expression.

In the lung, where BMP signaling has been linked to axial patterning of epithelial proliferation and differentiation of the developing bronchiole (Weaver et al., 2000), *Noggin* and *Bmp4* expression have been correlated with inductive signaling by SHH (Weaver et al., 2003) and within the context of the developing prostate duct, *Shh* and *Noggin* expression do occur in apparently complementary patterns. Epithelial *Shh* expression was concentrated at the duct tip while mesenchymal *Noggin* expression was concentrated in UGS mesenchyme around the duct tip. While suggestive of an inductive relationship, we have been unable to show a direct inductive effect. We could not demonstrate a direct effect of SHH on *Noggin* expression in UGSM-2 cells (unpublished observations) nor could we show a change in *Noggin* expression in SHH-treated UGS cultured *in vitro.* In fact, we observed a surprising increase in *Noggin* expression when the cultured UGS was treated with the hedgehog inhibitor cyclopamine. These

observations do not exclude an interdependency of *Shh* and *Noggin* expression, but argue against a simple, direct inductive relationship. In contrast, BMP4 does exert a clear inductive effect on *Noggin* expression. This was demonstrated in both UGS organ culture and in a UGS mesenchymal cell based assay, arguing that this is a direct effect of BMP4 on UGS mesenchyme that does not require crosstalk between mesenchyme and epithelium. Similar inductive relationships have been observed in other systems (Nakamura et al., 2005; Pujades et al., 2006; Stottmann et al., 2001). The complementary gradients of mesenchymal *Bmp4* and *Noggin* expression along the duct axis could result from inductive interactions superimposed on the physical displacement associated with bud outgrowth. Alternatively, it could suggest that the inductive relationship is modified by other factors such as SHH or FGF10.

We expected that *Noggin* loss of function would incur significant disruptions of epithelial proliferation and differentiation during development *in vivo*. We were therefore very surprised by the preservation of ductal architecture and epithelial cell populations in rescued grafts of the *Noggin*$^{-/-}$ UGS. It is possible that the perturbations introduced by *Noggin* loss of function are muted by compensatory changes in *Bmp* ligand expression and/or altered expression of other inhibitory ligands such as *Gremlin* that provide a measure of functional redundancy (Merino et al., 1999). Indeed, we have recently demonstrated that *Shh* loss of function is mitigated, in part, by functional compensation achieved through increased expression of *Ihh* (Doles et al., 2006). In an effort to circumvent these issues, we used shorter-term culture and a pulse-chase strategy to dissect out the influence of NOGGIN on prostatic budding and proliferation in UGS organ culture. These studies clearly showed that BMP4 specifically inhibited the proliferation of P63+ cells concentrated at the tips of nascent prostatic buds and that this effect is completely reversed by NOGGIN. These studies complement our finding that inhibition of ductal budding by exogenous is similarly blocked by NOGGIN and leads us to postulate that NOGGIN acts to specifically inhibit BMP4/7 activity during ductal budding and promote P63+ cell proliferation at tip of the nascent duct to facilitate outgrowth and simultaneously create a gradient of BMP signaling along the ductal axis. The lack of proliferation effect of NOGGIN exposure for one day without BMP4 pre-treatment suggests that endogenous BMP activity has already been neutralized by endogenous BMP-antagonist activity, an activity consistent with the concentrated expression of Noggin around the growing duct tip.

Noggin$^{-/-}$ mice exhibit specific abnormalities of prostate development including generalized deficiency of prostatic buds and specific loss of VP development. Since exogenous BMP4 or BMP7 added to UGS and prostate organ cultures caused a global dose-dependent reduction in prostatic buds (Grishina et al., 2005; Lamm et al., 2001), the generalized deficiency of prostatic budding is likely caused by unopposed BMP signaling from the actions of BMP4 and BMP7. Against a generalized inhibition of ductal budding, the loss of VP development in the *Noggin*$^{-/-}$ mutant appears to be a uniquely specific effect. Not only was there complete loss of ventral budding in all mutants examined, but there was deficiency or absence of the ventral mesenchymal pad. The absence of the ventral mesenchymal pad correlates with a deficit in proliferation in the ventral epithelium at E14. Since the lobe-specificity of epithelial differentiation is determined by the identity of the inductive mesenchyme, the absence of ventral mesenchyme explains the complete absence of VP differentiation in rescued null grafts. This contrasts with the observed absence of morphologically identifiable CG buds but the unequivocal presence of CG differentiation marker expression in the grafted tissues. While the *Noggin*$^{-/-}$ UGS was approximately half the size of the WT UGS at E14, the renal grafts were of roughly equal size. One possible explanation is that the absence of *Noggin* alters patterning of the UGS mesenchyme and lobar identity, but does not change the overall growth potential of the prostate. An alternative explanation is that *Noggin* may be expressed by the host mouse at the graft site and provide functional compensation. In fact, we have shown that *Noggin* is

expressed by host stromal cells in LNCaP xenograft tumors and is upregulated by Shh overexpression (unpublished observations).

Axial development of the male accessory sex organs follows a sequential cascade from cranial to caudal (Altmann and Brivanlou, 2001; Kmita and Duboule, 2003; Podlasek et al., 1999a; Podlasek et al., 1999b; Warot et al., 1997). Since the VP is the most caudal structure of the prostate, one possible explanation for VP agenesis in *Noggin*$^{-/-}$ mice is that unopposed BMP signaling in the developing fetus causes generalized caudal agenesis. We considered the possibility that VP agenesis is not a prostate lobe-specific effect but rather a manifestation of generalized caudal agenesis that affects the VP specifically because it is the most caudal of the prostate lobes. Although we did observe diminished proliferation in the ventral mesenchyme of the *Noggin*$^{-/-}$ mutant, we do not favor this interpretation because the uniform absence of the ventral prostate in all KO's examined contrasts with the inconsistent agenesis of even more caudal urogenital structures such as the membraneous urethra or bulbourethral gland. This suggests some specificity in the effect on the VP beyond its relative caudal position. A selective effect on VP development could result if there is functional compensation for loss of *Noggin* in the other regions of the UGS or greater BMP expression in the ventral region compared to other regions of the UGS. Alternatively, VP agenesis could result from an altered patterning of the UGS if NOGGIN-mediated neutralization of BMP activity is required to specify development of the ventral mesenchymal pad and pattern ventral budding The failure to restore VP development by in vitro organ culture with exogenous NOGGIN may indicate that NOGGIN's role in VP determination occurs prior to E12 or that proper specification of VP development requires localized NOGGIN activity that cannot be mimicked by addition to the media. Recently, *Bmp4* haploinsuffiency was shown to partially rescue lung development in *Noggin*$^{-/-}$ mice suggesting that the balance of BMP/NOGGIN activity is a critical regulator of cell proliferation and differentiation (Que et al., 2006). It is possible that a similar rescue of VP prostate could be obtained by haploinsufficiency for *Bmp4* and/or *Bmp7*. However, VP determination appears to be influenced by a multiplicity of factors, including members of the *Hox* gene family, retinoic acid and aryl hydrocarbon receptor ligands and it is possible that the effect of NOGGIN loss of function occurs from upstream effects on these other pathways as well as direct effects on VP mesenchyme proliferation.

Supplementary Material

Refer to Web version on PubMed Central for supplementary material.

Acknowledgements

The authors would like to thank Brigid Hogan for supplying a breeder pair of *Noggin*$^{tm1(Lacz)Am}$ mice, Edward DeRobertis for supplying the *Chordin* knockout mice, the UW Flow Cytometry Lab for its use of the fluorescence microscope, Jerry Gipp and Rob Lipinski for their contributions to the cell regulation studies and mouse colony maintenance, and Xin Sun (UW-Madison) for providing the mouse *Noggin* cDNA and Gremlin knockout mice. This work was supported by the following Peterson Lab grants: NIH P50 DK065303, NIH R37 ES01332, F32 ES014284, and F31 HD049323 and Bushman Lab grants: NIH P50 DK052687, NIH O'Brien DK065303, and DOD W81XWH.

References

Almahbobi G, Hedwards S, Fricout G, Jeulin D, Bertram JF, Risbridger GP. Computer-based detection of neonatal changes to branching morphogenesis reveals different mechanisms of and predicts prostate enlargement in mice haploinsufficient for bone morphogenetic protein 4. J Pathol 2005;206:52–61. [PubMed: 15772937]

Altmann CR, Brivanlou AH. Neural patterning in the vertebrate embryo. Int Rev Cytol 2001;203:447–82. [PubMed: 11131523]

Balemans W, Van Hul W. Extracellular regulation of BMP signaling in vertebrates: a cocktail of modulators. Dev Biol 2002;250:231–50. [PubMed: 12376100]

Berman DM, Desai N, Wang X, Karhadkar SS, Reynon M, Abate-Shen C, Beachy PA, Shen MM. Roles for Hedgehog signaling in androgen production and prostate ductal morphogenesis. Dev Biol 2004;267:387–98. [PubMed: 15013801]

Cheng TC, Wallace MC, Merlie JP, Olson EN. Separable regulatory elements governing myogenin transcription in mouse embryogenesis. Science 1993;261:215–8. [PubMed: 8392225]

Cunha GR, Donjacour AA, Cooke PS, Mee S, Bigsby RM, Higgins SJ, Sugimura Y. The endocrinology and developmental biology of the prostate. Endocr Rev 1987;8:338–62. [PubMed: 3308446]

Doles J, Cook C, Shi X, Valosky J, Lipinski R, Bushman W. Functional compensation in Hedgehog signaling during mouse prostate development. Dev Biol. 2006

Doles JD, Vezina CM, Lipinski RJ, Peterson RE, Bushman W. Growth, morphogenesis, and differentiation during mouse prostate development in situ, in renal grafts, and in vitro. Prostate 2005;65:390–9. [PubMed: 16114054]

Donjacour AA, Thomson AA, Cunha GR. FGF-10 plays an essential role in the growth of the fetal prostate. Dev Biol 2003;261:39–54. [PubMed: 12941620]

Freestone SH, Marker P, Grace OC, Tomlinson DC, Cunha GR, Harnden P, Thomson AA. Sonic hedgehog regulates prostatic growth and epithelial differentiation. Dev Biol 2003;264:352–62. [PubMed: 14651923]

Gao N, Ishii K, Mirosevich J, Kuwajima S, Oppenheimer SR, Roberts RL, Jiang M, Yu X, Shappell SB, Caprioli RM, Stoffel M, Hayward SW, Matusik RJ. Forkhead box A1 regulates prostate ductal morphogenesis and promotes epithelial cell maturation. Development 2005;132:3431–43. [PubMed: 15987773]

Garrett WM, G HD. Detection of Bromodeoxyuridine in Paraffin-embedded Tissue Sections Using Microwave Antigen Retrieval is Dependent on the Mode of Tissue Fixation. Biochemica 1998;No. 1:17–20.

Grishina IB, Kim SY, Ferrara C, Makarenkova HP, Walden PD. BMP7 inhibits branching morphogenesis in the prostate gland and interferes with Notch signaling. Dev Biol 2005;288:334–47. [PubMed: 16324690]

Hayashi N, Cunha GR, Parker M. Permissive and instructive induction of adult rodent prostatic epithelium by heterotypic urogenital sinus mesenchyme. Epithelial Cell Biol 1993;2:66–78. [PubMed: 8353595]

Huang L, Pu Y, Alam S, Birch L, Prins GS. The role of Fgf10 signaling in branching morphogenesis and gene expression of the rat prostate gland: lobe-specific suppression by neonatal estrogens. Dev Biol 2005;278:396–414. [PubMed: 15680359]

Hynes PJ, Fraher JP. The development of the male genitourinary system. I. The origin of the urorectal septum and the formation of the perineum. Br J Plast Surg 2004;57:27–36. [PubMed: 14672675]

Jeffery TK, Upton PD, Trembath RC, Morrell NW. BMP4 inhibits proliferation and promotes myocyte differentiation of lung fibroblasts via Smad1 and JNK pathways. Am J Physiol Lung Cell Mol Physiol 2005;288:L370–8. [PubMed: 15516492]

Khokha MK, Hsu D, Brunet LJ, Dionne MS, Harland RM. Gremlin is the BMP antagonist required for maintenance of Shh and Fgf signals during limb patterning. Nat Genet 2003;34:303–7. [PubMed: 12808456]

Kmita M, Duboule D. Organizing axes in time and space; 25 years of colinear tinkering. Science 2003;301:331–3. [PubMed: 12869751]

Lamm ML, Catbagan WS, Laciak RJ, Barnett DH, Hebner CM, Gaffield W, Walterhouse D, Iannaccone P, Bushman W. Sonic hedgehog activates mesenchymal Gli1 expression during prostate ductal bud formation. Dev Biol 2002;249:349–66. [PubMed: 12221011]

Lamm ML, Podlasek CA, Barnett DH, Lee J, Clemens JQ, Hebner CM, Bushman W. Mesenchymal factor bone morphogenetic protein 4 restricts ductal budding and branching morphogenesis in the developing prostate. Dev Biol 2001;232:301–14. [PubMed: 11401393]

Lin TM, Rasmussen NT, Moore RW, Albrecht RM, Peterson RE. Region-specific inhibition of prostatic epithelial bud formation in the urogenital sinus of C57BL/6 mice exposed in utero to 2,3,7,8-tetrachlorodibenzo-p-dioxin. Toxicol Sci 2003;76:171–81. [PubMed: 12944588]

McMahon JA, Takada S, Zimmerman LB, Fan CM, Harland RM, McMahon AP. Noggin-mediated antagonism of BMP signaling is required for growth and patterning of the neural tube and somite. Genes Dev 1998;12:1438–52. [PubMed: 9585504]

Merino R, Rodriguez-Leon J, Macias D, Ganan Y, Economides AN, Hurle JM. The BMP antagonist Gremlin regulates outgrowth, chondrogenesis and programmed cell death in the developing limb. Development 1999;126:5515–22. [PubMed: 10556075]

Mills JS, Needham M, Thompson TC, Parker MG. Androgen-regulated expression of secretory protein synthesis in mouse ventral prostate. Mol Cell Endocrinol 1987;53:111–8. [PubMed: 3666286]

Nakamura Y, Wakitani S, Saito N, Takaoka K. Expression profiles of BMP-related molecules induced by BMP-2 or -4 in muscle-derived primary culture cells. J Bone Miner Metab 2005;23:426–34. [PubMed: 16261448]

Podlasek CA, Clemens JQ, Bushman W. Hoxa-13 gene mutation results in abnormal seminal vesicle and prostate development. J Urol 1999a;161:1655–61. [PubMed: 10210434]

Podlasek CA, Seo RM, Clemens JQ, Ma L, Maas RL, Bushman W. Hoxa-10 deficient male mice exhibit abnormal development of the accessory sex organs. Dev Dyn 1999b;214:1–12. [PubMed: 9915571]

Pu Y, Huang L, Prins GS. Sonic hedgehog-patched Gli signaling in the developing rat prostate gland: lobe-specific suppression by neonatal estrogens reduces ductal growth and branching. Dev Biol 2004;273:257–75. [PubMed: 15328011]

Pujades C, Kamaid A, Alsina B, Giraldez F. BMP-signaling regulates the generation of hair-cells. Dev Biol 2006;292:55–67. [PubMed: 16458882]

Que J, Choi M, Ziel JW, Klingensmith J, Hogan BL. Morphogenesis of the trachea and esophagus: current players and new roles for noggin and Bmps. Differentiation 2006;74:422–37. [PubMed: 16916379]

Shaw A, Papadopoulos J, Johnson C, Bushman W. Isolation and characterization of an immortalized mouse urogenital sinus mesenchyme cell line. Prostate. 2006

Signoretti S, Pires MM, Lindauer M, Horner JW, Grisanzio C, Dhar S, Majumder P, McKeon F, Kantoff PW, Sellers WR, Loda M. p63 regulates commitment to the prostate cell lineage. Proc Natl Acad Sci U S A 2005;102:11355–60. [PubMed: 16051706]

Signoretti S, Waltregny D, Dilks J, Isaac B, Lin D, Garraway L, Yang A, Montironi R, McKeon F, Loda M. p63 is a prostate basal cell marker and is required for prostate development. Am J Pathol 2000;157:1769–75. [PubMed: 11106548]

Smith WC. TGF beta inhibitors. New and unexpected requirements in vertebrate development. Trends Genet 1999;15:3–5. [PubMed: 10087923]

Staack A, Donjacour AA, Brody J, Cunha GR, Carroll P. Mouse urogenital development: a practical approach. Differentiation 2003;71:402–13. [PubMed: 12969333]

Stottmann RW, Anderson RM, Klingensmith J. The BMP antagonists Chordin and Noggin have essential but redundant roles in mouse mandibular outgrowth. Dev Biol 2001;240:457–73. [PubMed: 11784076]

Thielen JL, Volzing KG, Collier LS, Green LE, Largaespada DA, Marker PC. Markers of prostate region-specific epithelial identity define anatomical locations in the mouse prostate that are molecularly similar to human prostate cancers. Differentiation 2007;75:49–61. [PubMed: 17244021]

Thomson AA. Role of androgens and fibroblast growth factors in prostatic development. Reproduction 2001;121:187–95. [PubMed: 11226043]

Thomson AA, Cunha GR. Prostatic growth and development are regulated by FGF10. Development 1999;126:3693–701. [PubMed: 10409514]

Tomlinson DC, Freestone SH, Grace OC, Thomson AA. Differential effects of transforming growth factor-beta1 on cellular proliferation in the developing prostate. Endocrinology 2004;145:4292–300. [PubMed: 15192047]

Wang XD, Leow CC, Zha J, Tang Z, Modrusan Z, Radtke F, Aguet M, de Sauvage FJ, Gao WQ. Notch signaling is required for normal prostatic epithelial cell proliferation and differentiation. Dev Biol 2006;290:66–80. [PubMed: 16360140]

Wang XD, Shou J, Wong P, French DM, Gao WQ. Notch1-expressing cells are indispensable for prostatic branching morphogenesis during development and regrowth following castration and androgen replacement. J Biol Chem 2004;279:24733–44. [PubMed: 15028713]

Warot X, Fromental-Ramain C, Fraulob V, Chambon P, Dolle P. Gene dosage-dependent effects of the Hoxa-13 and Hoxd-13 mutations on morphogenesis of the terminal parts of the digestive and urogenital tracts. Development 1997;124:4781–91. [PubMed: 9428414]

Weaver M, Batts L, Hogan BL. Tissue interactions pattern the mesenchyme of the embryonic mouse lung. Dev Biol 2003;258:169–84. [PubMed: 12781691]

Weaver M, Dunn NR, Hogan BL. Bmp4 and Fgf10 play opposing roles during lung bud morphogenesis. Development 2000;127:2695–704. [PubMed: 10821767]

Wijgerde M, Karp S, McMahon J, McMahon AP. Noggin antagonism of BMP4 signaling controls development of the axial skeleton in the mouse. Dev Biol 2005;286:149–57. [PubMed: 16122729]

Zimmerman LB, De Jesus-Escobar JM, Harland RM. The Spemann organizer signal noggin binds and inactivates bone morphogenetic protein 4. Cell 1996;86:599–606. [PubMed: 8752214]

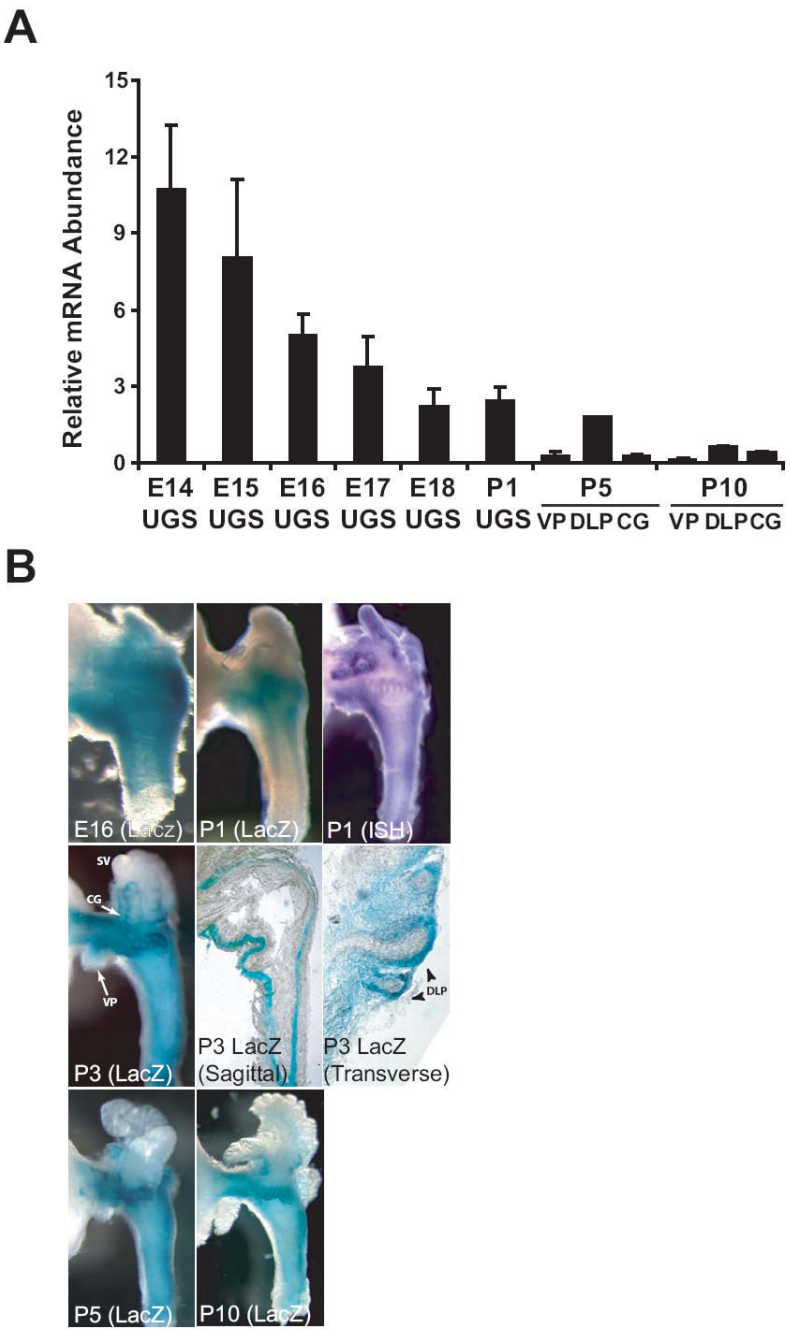

Figure 1. Temporal and spatial expression of *Noggin* in the developing UGS and prostate of male mice

(A) To assess the temporal expression of *Noggin* during prostate development, whole UGS from embryonic male mice and isolated ventral prostate (VP), dorsolateral prostate (DLP) and coagulating gland (GC) of postnatal male mice were collected at regular intervals during development (E14-P10). RNA was isolated from pooled UGS tissues (n = 6-9 E14-18 male fetuses from multiple litters) or individual prostate tissues from P1-P10 male neonates. *Noggin* mRNA abundance was determined by real-time PCR and normalized to glyceraldehyde phosphate dehydrogenase gene expression. Results are the mean (± SEM) of two RNA pools for E14-18 UGS, or three separate prostates (P1-P10. (B) Temporal and spatial expression of

the *Noggin*$^{tm1(Lacz)Am}$ transgene in developing UGS and prostate from *Noggin*$^{+/-}$ transgenic mice. UGS or prostate tissues were removed from male mice at different days during gestation and postnatal development and probed for *Noggin*$^{tm1(Lacz)Am}$-mediated β-galactosidase activity or *Noggin* mRNA expression by whole-mount ISH. Photographs are representative of $n > 10$ UGS specimens. To visualize the global expression of *Noggin* as well as its expression in specific prostate structures, β-galactosidase activity in UGS specimens from P3 mice was visualized by whole mount imaging (left, center row), imaging of sagittal sections cut along the caudal-cranial urethral axis (center, center row), and imaging of transverse sections cut along the lateral-medial urethral axis (right, center row). *Noggin* expression was observed in mesenchyme surrounding seminal vesicles and prostatic buds of the VP, DLP, and CG in P1-10 mouse prostate. *Noggin* expression was most concentrated at distal tips of individual nascent DLP buds and decreased proximally towards the base of buds (right, center row).

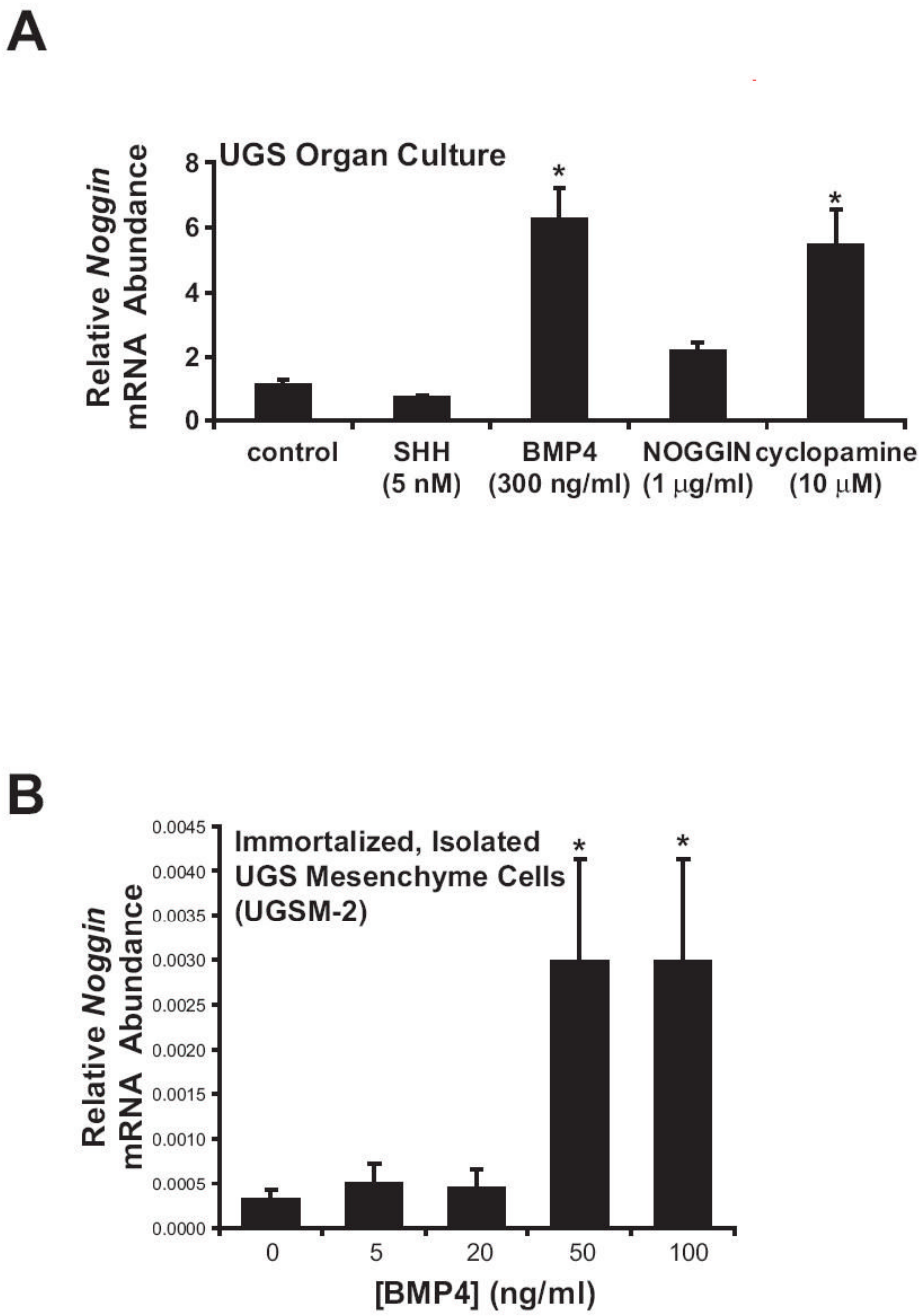

Figure 2. Regulation of *Noggin* expression in the UGS

(A) To assess the regulatory relationship between NOGGIN, SHH, and BMP4, UGSs from E14 WT male mice were exposed in organ culture to recombinant octylated SHH (5 nM), BMP4 (300 ng/ml), NOGGIN (1 μg/ml), the hedgehog inhibitor cyclopamine (10 μM) or vehicle (0.1% BSA, control) for 3 days and the relative abundance of *Noggin* mRNA was determined for individual cultured UGS tissues by real-time RT-PCR. Results are mean (± s.e.m.), $n \geq 5$ UGS specimens. (B) To determine whether BMP4-mediated induction of *Noggin* mRNA was caused by these agents acting directly on UGS mesenchyme, the UGSM-2 cell line (Shaw et al., 2006) was exposed to vehicle (0.01% BSA) or recombinant BMP4 for 24 hours and the expression of *Noggin* mRNA mean (± s.e.m.) was evaluated by real-time RT-

PCR from three independent experiments. Significant differences between groups were determined by Analysis of Variance (ANOVA), followed by the Fisher Least Significant Difference post-hoc test. “*” Indicates significantly different from vehicle-exposed control UGS ($p < 0.01$).

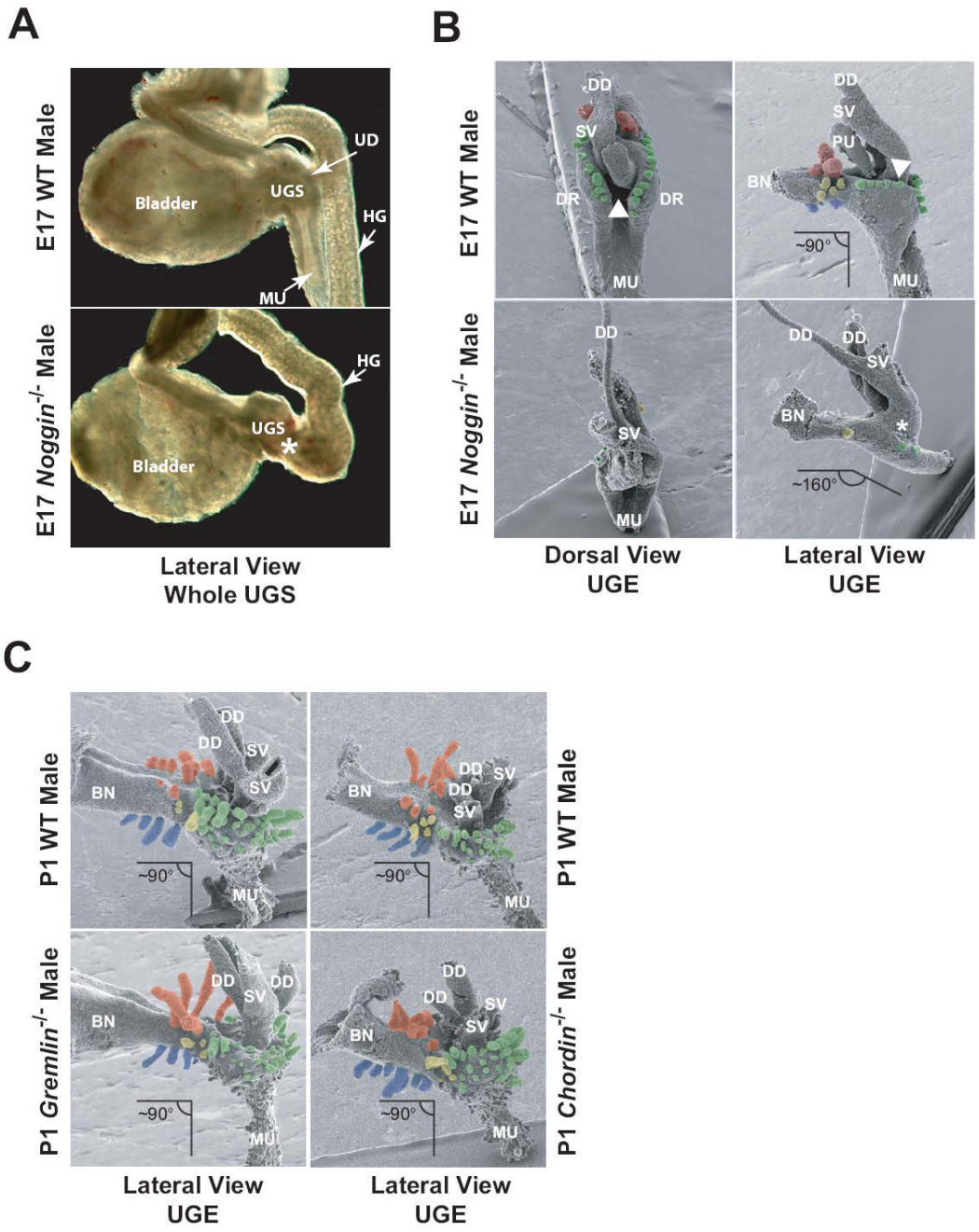

Figure 3. Phenotype of the developing prostate from *Noggin*$^{-/-}$ male mouse fetuses

(A) UGS/hindgut complexes from WT and *Noggin*$^{-/-}$ male mice were removed from representative E17 male mouse fetuses ($n = 3$ per genotype) and visualized by light microscopy. The urogenital division (UD) that separates the hindgut (HG) from the UGS in the WT specimen was absent (denoted by "*") and the membranous portion of the urethra (MU) failed to elongate in the *Noggin*$^{-/-}$ mouse specimen. (B) To better visualize the overall architecture of the *Noggin*$^{+/+}$ and *Noggin*$^{-/-}$ UGS, UGS epithelium (UGE) was separated from mesenchyme and visualized by scanning electron microscopy (SEM). Isolated UGE of a representative WT E17 male fetus ($n = 3$) revealed seminal vesicles (SV) and ductus deferens (DD) that drained into the ejaculatory duct located within the dorsal sulcus (white arrowhead), or groove, created

by two prominent dorsal ridges (DR) on the lateral surfaces of the UGS. Emerging VP (blue), dorsal (green), lateral (yellow) CG (red) buds, and the prostatic utricle (PU) were also evident. On the other hand, VP buds and the PU were missing, DLP and CG budding was reduced, and the ejaculatory ducts were laterally displaced and drained into the DR instead of the dorsal sulcus (*) in the representative *Noggin*$^{-/-}$ UGS. Also, the angle between the bladder neck and urethra of WT UGS approximated 90°, whereas this angle was closer to 160° in the *Noggin*$^{-/-}$ UGS. (C) SEM images of *Gremlin*$^{-/-}$ and *Chordin*$^{-/-}$ male mouse prostate at P1 reveal budding patterns and prostate architecture that is very similar to WT littermates.

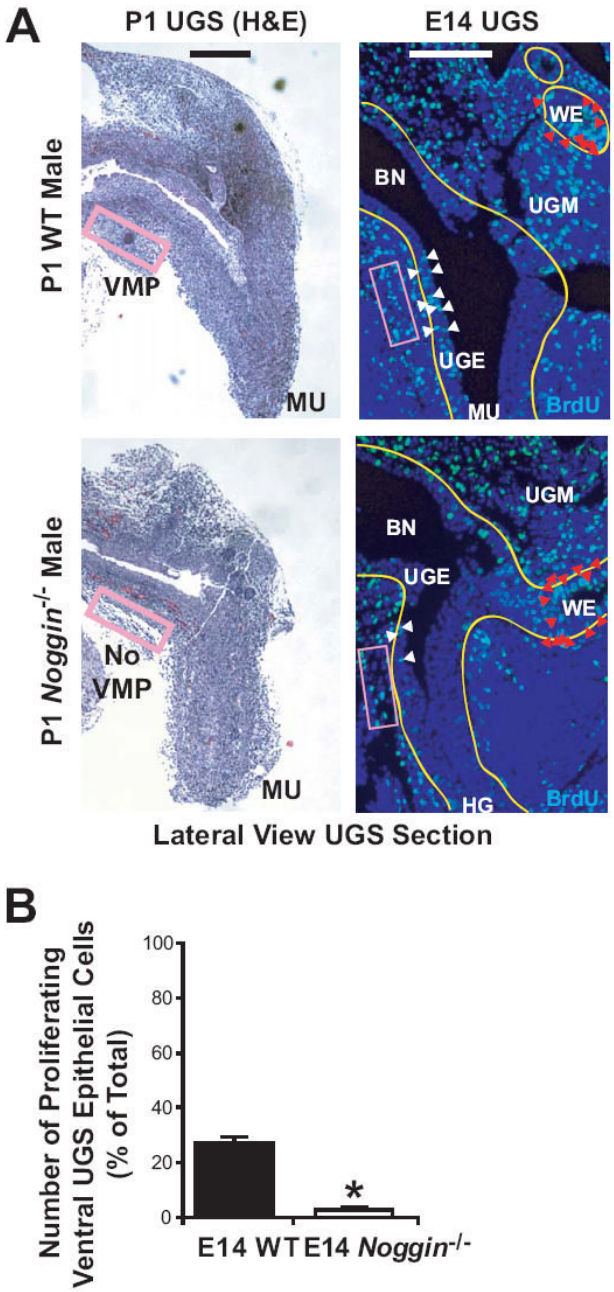

Figure 4. *Noggin* is required for formation of the ventral mesenchymal pad and for ventral UGS epithelial cell proliferation

(A, left column) Representative H&E stained prostate tissue sections (n = 5 per genotype) of P1 mouse prostate indicating thinning or absence of the ventral mesenchymal pad (VMP) in the P1 *Noggin*$^{-/-}$ prostate. (A, right column) E14 WT and *Noggin*$^{-/-}$ UGS were labeled in utero with BrdU 2 hr prior to euthanasia, sectioned and stained to evaluate epithelial cell proliferation. Representative photomicrographs (n = 3 UGS per genotype) from WT and *Noggin*$^{-/-}$ UGS reveals decreased ventral UGS mesenchymal cell (UGM) density (outlined in pink) and fewer proliferating ventral UGS epithelial cells (UGE; white arrowheads), while cell proliferation in the Wolffian-derived epithelium (WE) was comparable between groups. (B) Proliferating

ventral UGS epithelial cells (% of total) were quantified from a fixed area within 3-6 sections per UGS (3 UGS per genotype). Results are expressed as mean (± s.e.m.), $n = 3$. Significant differences between groups were determined by Student's T test. "*" Indicates significantly different from WT ($p < 0.05$). Scale bar = 100 μm.

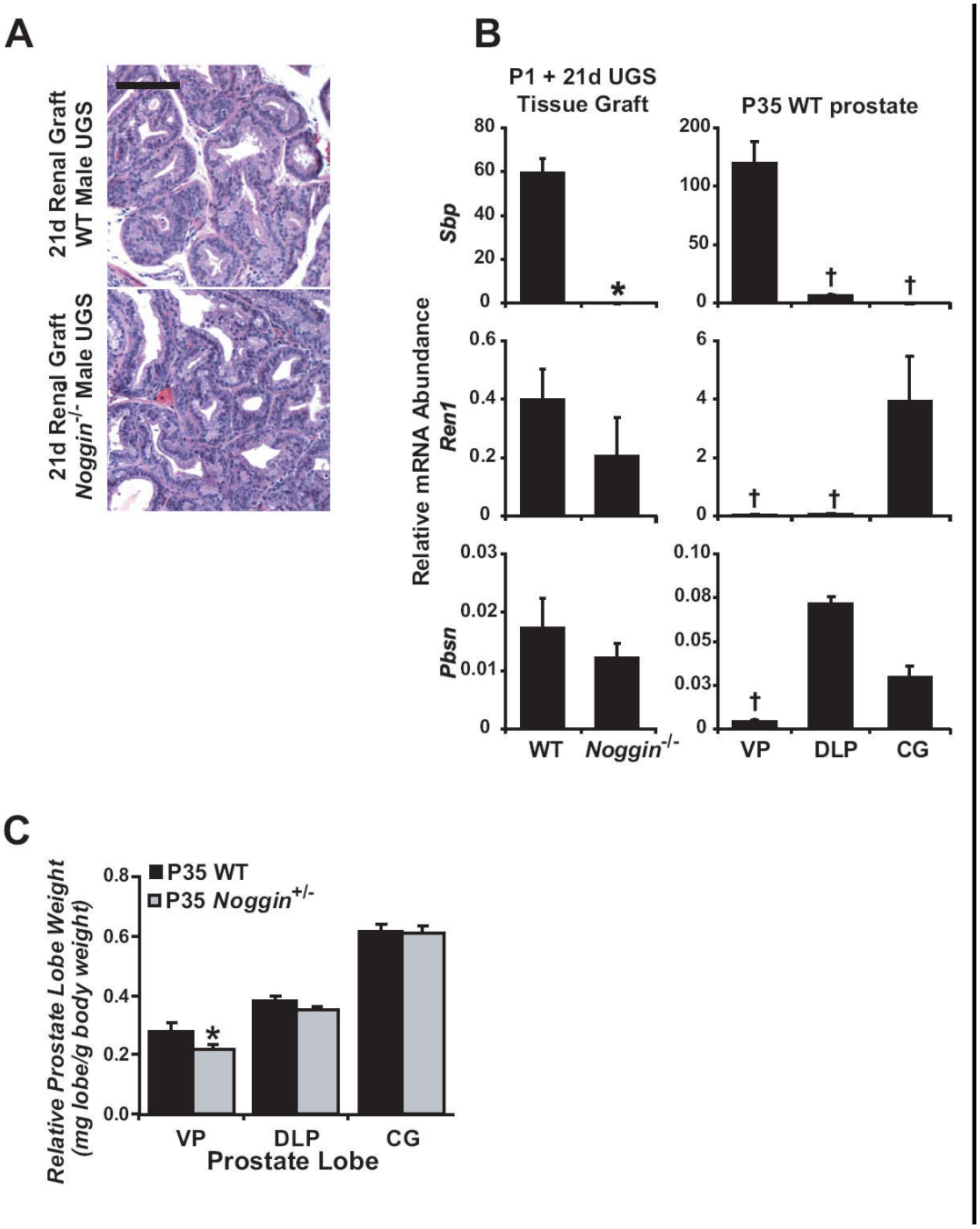

Figure 5. Ventral prostate development is inhibited in *Noggin*$^{-/-}$ male mice

To determine if UGSs from *Noggin*$^{-/-}$ male mice are capable of supporting development and differentiation into mature prostate tissue, prostates from WT, *Noggin*$^{+/-}$, and *Noggin*$^{-/-}$ P1 newborn mice were grafted under the kidney capsule of nude mice for 21 days. (A) Hematoxylin and eosin stained graft sections of WT and *Noggin*$^{-/-}$ mice revealed a ductal network characteristic of mature prostate containing prostatic secretions. There were no qualitative differences in the dorsolateral prostate ductal structure of WT and *Noggin*$^{-/-}$ UGS renal grafts. Scale bar = 100 μm. (B) Prostate lobe-specific marker abundance was compared between the WT and *Noggin*$^{-/-}$ prostate renal grafts. Results are expressed as mean (± s.e.m.), $n = 3$. Significant differences between groups were determined by Student's T test. "*"

Indicates significantly different from WT ($p < 0.05$). Specificity of *Sbp*, *Ren1*, and *Pbsn* expression for VP, CG, and DLP, respectively, was established by comparing the relative mRNA abundance of each message in prostate tissue from P35 WT mice. Results are expressed as mean (± s.e.m.), $n = 3$. Significant differences between groups were determined by ANOVA followed by the Fisher Least Significant Difference post-hoc test. †" Indicates significantly different from VP, CG, and DLP, for *Sbp*, *Ren1*, and *Pbsn*, respectively ($p < 0.05$). Significant differences between groups were determined by Student's T test. ((C) To determine whether *Noggin*$^{+/-}$ mice exhibited a haploinsufficient phenotype, P35 WT and *Noggin*$^{+/-}$ prostate lobe weights for were measured and normalized to total body weight. Results are mean (± s.e.m.), $n \geq 18$ for each genotype. "*" Indicates significantly different from WT ($p < 0.05$).

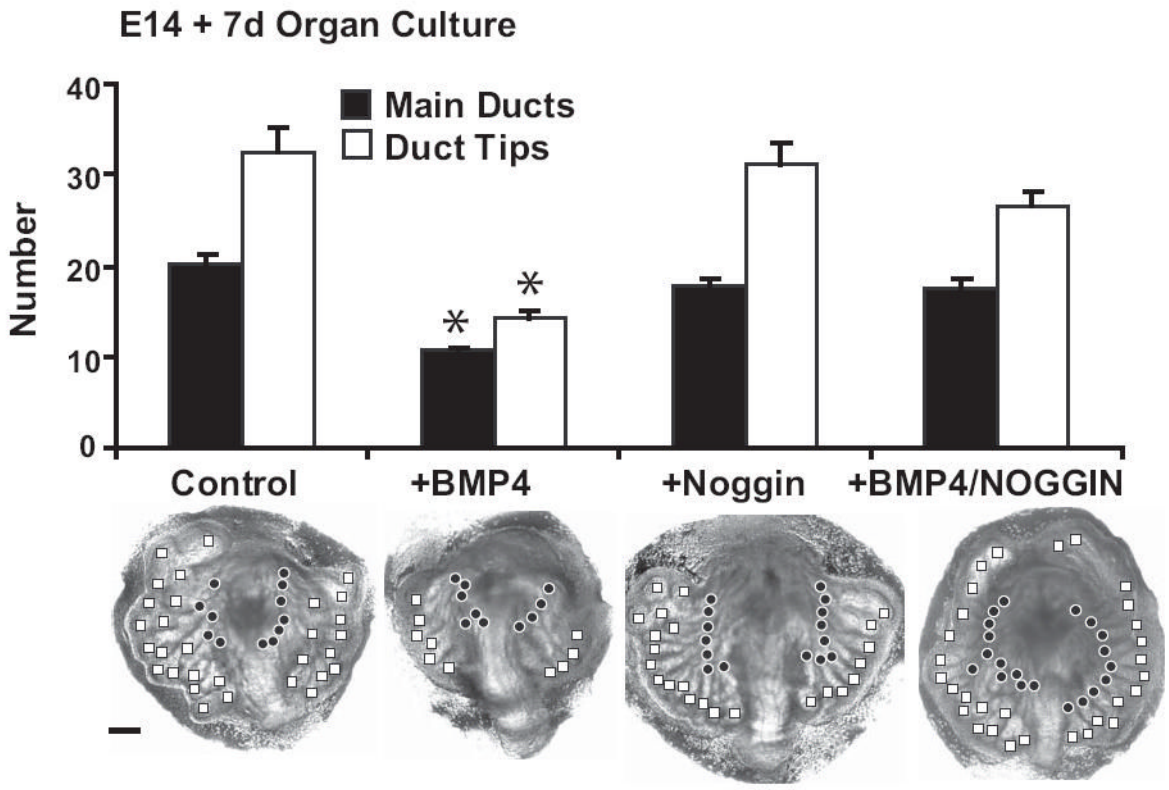

Figure 6. Effect of NOGGIN on prostatic budding, branching, and cell proliferation in UGS or neonatal prostate organ culture

To determine whether exposure to recombinant NOGGIN and/or recombinant BMP4 alters prostatic budding or E14 WT UGS was incubated for 7 days in organ culture containing vehicle (0.01% BSA; control), recombinant BMP4 (300 ng/ml), recombinant NOGGIN (1 μg/ml) or a combination of NOGGIN and BMP4. (A) The number of bud tips (□) and main ducts (●) per UGS were determined. Results are mean (± s.e.m.), $n \geq 10$ samples per group. Significant differences between groups were determined by ANOVA, followed by the Fisher Least Significant Difference test. "*" Indicates significantly different from control ($p < 0.001$). Representative UGS samples after 7 days in organ culture are shown for each treatment group.

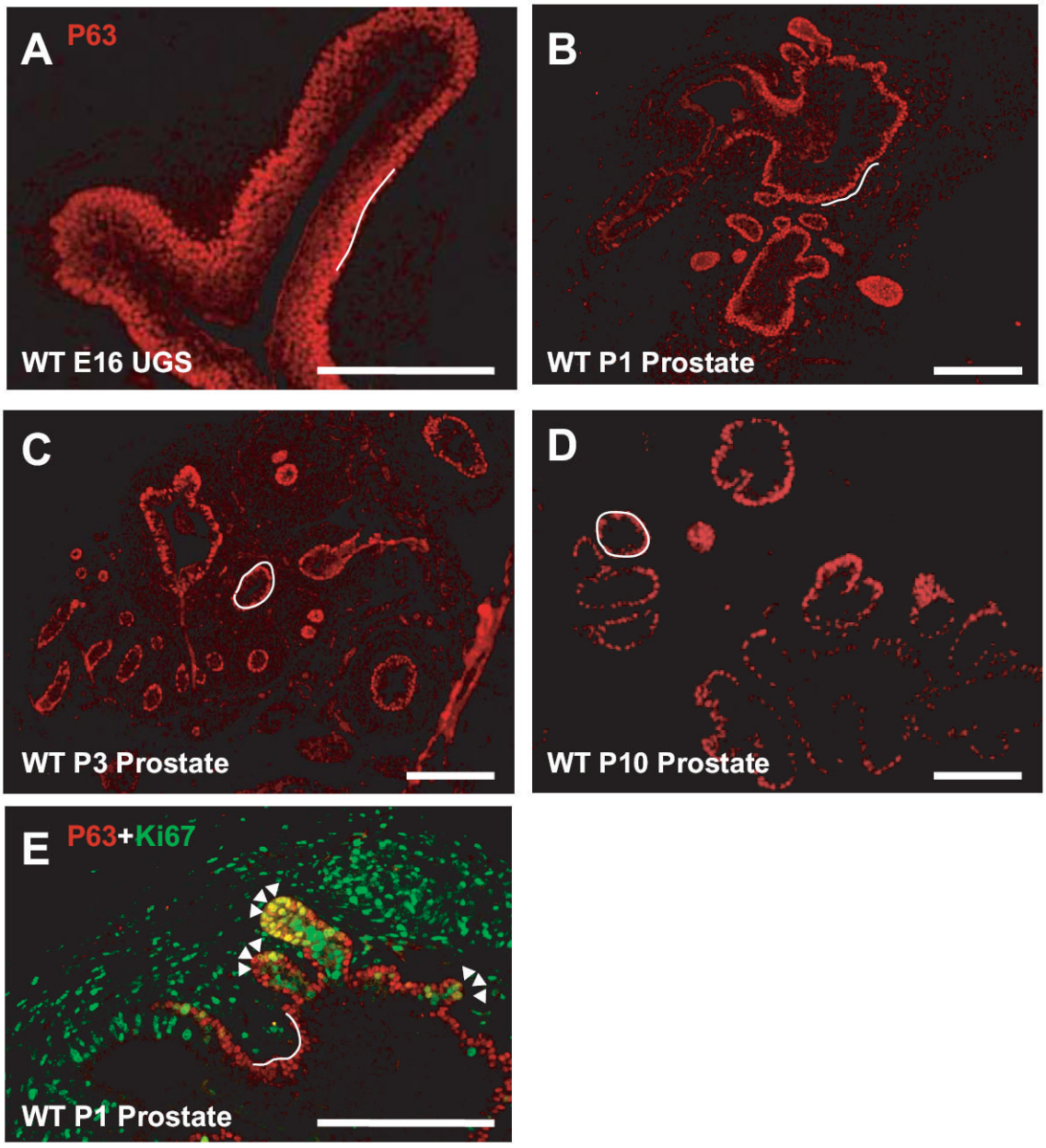

Figure 7. Ontogeny of P63 expresssion in developing WT UGS and early postnatal prostate

CD-1 mouse UGS and prostate tissue specimens were analyzed for P63 expression by immunohistochemistry. (A) Multiple layers of P63-positive staining basal epithelial cells accumulated beneath the basal lamina (partially contoured in white) of the UGS and urethra at E16 in WT male mice. (B-E) During postnatal development from P1-P10, P63 expression was gradually restricted to a single P63+ epithelial cell layer beneath the basal lamina of developing prostate ducts. (E) Immunohistochemical analysis of P63 and Ki67 expression in prostate sections from P1 WT male newborn mice revealed numerous P63+ basal epithelial cells (red) throughout prostatic epithelium, including prostate buds. Ki67-positive cells (green) were observed in prostatic mesenchyme and prostate epithelium. P63+, proliferating cells (yellow) in prostate epithelium were restricted to the tips of emerging prostate buds (arrowheads). Scale bar = 100 μm.

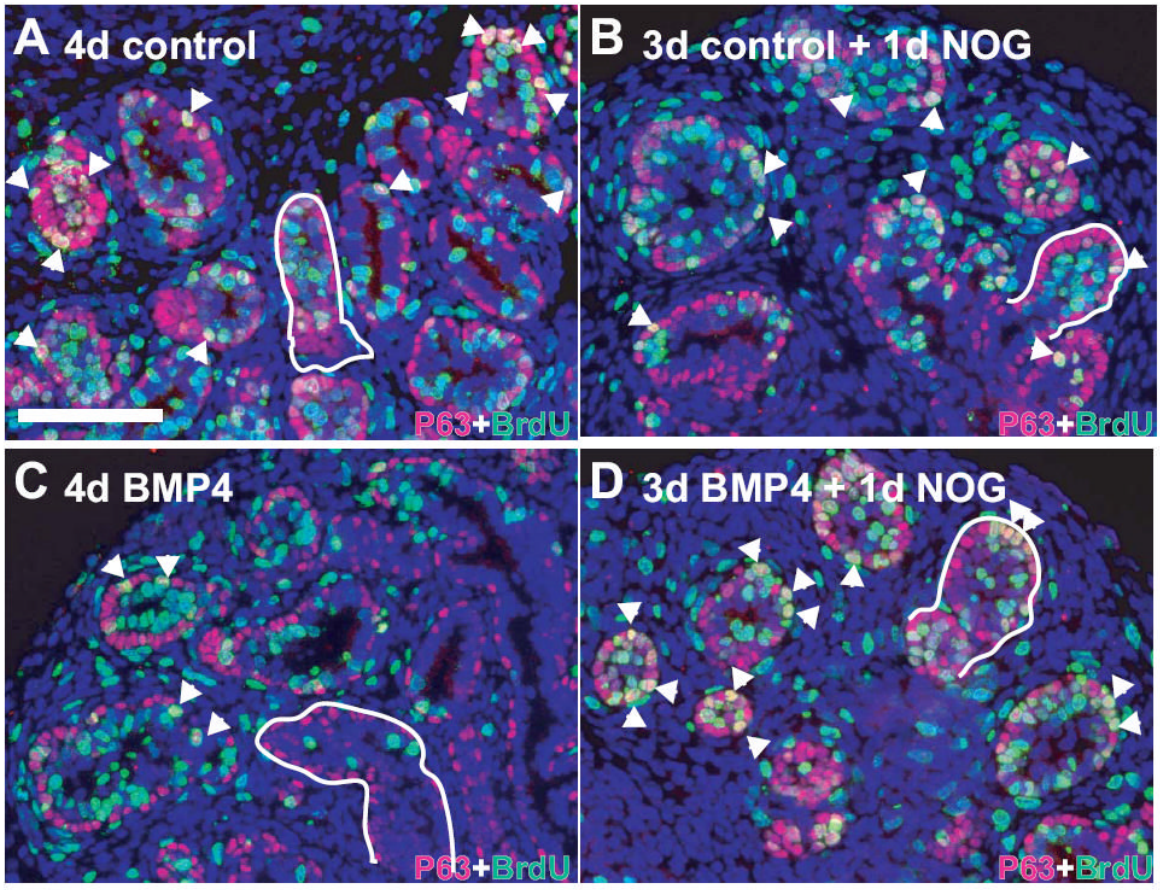

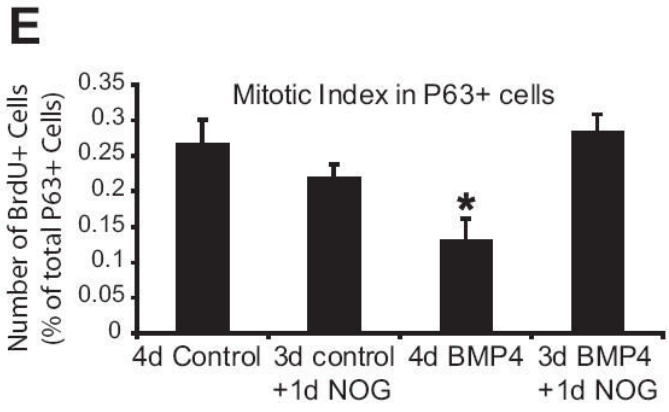

Figure 8. NOGGIN exposure induces proliferation of BMP4-exposed prostate in organ culture

P1 prostates were incubated for 3 days in organ culture with vehicle (0.1% BSA; control) or recombinant BMP4 (300 ng/ml). The organ culture media was then replaced with media containing vehicle, recombinant NOGGIN (1 μg/ml), or BMP4 and cultures were incubated for an additional day. Four hours before harvesting the tissue, BrdU was added to the media to stain proliferating cells. Tissue sections were then assayed for BrdU (green) and P63 (pink) expression by IHC. Prostatic buds are indicated by arrowheads and the basal lamina for one bud in panels A-D is traced in white. (A) Vehicle-exposed prostates showed proliferation in prostate mesenchyme and P63+ and P63- epithelial cells. (B) NOGGIN (NOG) exposure for 1 day does not change the proliferation of P63- epithelial cells within the core of prostatic buds

compared to control prostates. (C) BMP4 exposure for 4 days decreased proliferation of P63 + but not P63- epithelial cells compared to control. (D) BMP4 exposure for 3 days followed by NOGGIN exposure for 1 day caused a burst of proliferation in P63+ but not P63- epithelial cells at the leading edge of ducts. Scale bar = 100 μm. (E) Mitotic indices for P63+ cells were calculated by counting the number of proliferating, BrdU and P63 positive cells as a fraction of the total P63+ cell population for each treatment group. Results are the mean (± s.e.m) of 2 to 6 sections from each of four UGS specimens per treatment group. Differences between groups were determined by Fisher's protected least significant difference test. "*" indicates significantly different from control ($p < 0.05$). Analysis of mitotic indices for P63- cells revealed no differences between any of the treatment groups (not shown).

Table I

PCR primers for real-time RT-PCR analysis.

Genebank Accession #	Entrez Gene ID	Forward Primer	Reverse Primer
NM 008711	Noggin (*Nog*)	ACAGCGCCTGAGCAAGAAG	AGGTGCACAGACTTGGATGG
NM 007554	Bone Morphogenetic Protein 4 (*Bmp4*)	AATGTGACACGGTGGGAAAC	TGGGTGATGCTTGGGACTAC
NM 009170	Sonic Hedgehog (*Shh*)	GTGGAAGCAGGTTTCGACTG	GGTCCAGGAAGGTGAGGAAG
X06246	Microfibrillar associated protein 5 (*Sbp*)*	AGAGCCCAGAATGTCCTGGG	TTATCACGTGCTCTCCGTCC
U89840	Renin1 (*Ren1*)*	ACTCGGTGACTGTGGGTGG	AGGTGGGAACCCCTGTTGTAG
AK137501	Probasin (*Pbsn*)*	AAAGAGAAAGTACAGAGACA GG	AATGTACAGCGTATCATGGAC
NM 008907	peptidylprolyl isomerase A (*Ppia*)*	TCTCTCCGTAGATGGACCTG	ATCACGGCCGATGACGAGCC

*(From Lin et al., 2003)